

Balamuthia mandrillaris trophozoites ingest human neuronal cells via a trogocytosis-independent mechanism

Worakamol Pengsart

Faculty of Graduate Studies, Mahidol University, Nakhon Pathom, Thailand

Nongnat Thongkrachang

Siriraj Integrative Center for Neglected Parasitic Diseases, Department of Parasitology, Faculty of Medicine Siriraj Hospital, Mahidol University, Bangkok, Thailand

Narisara Whangviboonkij

Siriraj Integrative Center for Neglected Parasitic Diseases, Department of Parasitology, Faculty of Medicine Siriraj Hospital, Mahidol University, Bangkok, Thailand

Patsharaporn Techasintana Sarasombath

Siriraj Integrative Center for Neglected Parasitic Diseases, Department of Parasitology, Faculty of Medicine Siriraj Hospital, Mahidol University, Bangkok, Thailand

Kasem Kulkeaw (✉ kasem.kuk@mahidol.edu)

Siriraj Integrative Center for Neglected Parasitic Diseases, Department of Parasitology, Faculty of Medicine Siriraj Hospital, Mahidol University, Bangkok, Thailand

Research Article

Keywords: *Balamuthia mandrillaris*, SH-SY5Y, three-dimensional imaging, trogocytosis

Posted Date: March 11th, 2022

DOI: <https://doi.org/10.21203/rs.3.rs-1429887/v1>

License: © ⓘ This work is licensed under a Creative Commons Attribution 4.0 International License.

[Read Full License](#)

Abstract

Background: Environmental protozoa need an adaptation mechanism to survive drastic changes in niches in the human body. In the brain parenchyma, *Balamuthia mandrillaris* trophozoites, which are causative agents of fatal brain damage, must acquire nutrients through ingestion of the surrounding cells. However, the mechanism the trophozoites deploy for cellular uptake remains unknown.

Methods: Amoebic ingestion of human neural cell components was investigated using a coculture of clinically isolated *B. mandrillaris* trophozoites with human neuroblastoma SH-SY5Y cells. Cell-to-cell interactions were visualized in a three-dimensional manner using a confocal and holotomographic microscope.

Results: The *B. mandrillaris* trophozoites attached themselves to human neuroblastoma SH-SY5Y cells, followed by twisting themselves around the cytoplasmic bridge. Based on fluorescence-based cell tracking, the *B. mandrillaris* trophozoites inserted invadopodia into the cytoplasm of the human cells. Subsequently, the human protein-enriched components were internalized into the trophozoites in the form of nonmembranous granules, whereas the human lipids were dispersed in the cytoplasm. Intervention of trogocytosis, a process involving nibbling on the parts of target cells, failed to inhibit this cellular uptake.

Conclusions: In summary, human cell ingestion by *B. mandrillaris* trophozoites likely differs from trogocytosis, suggesting that a pathogen-specific strategy can be used to ameliorate brain damage.

Background

The adaptability of single-cell organisms to different habitats plays a role in biological fitness. From the environment to the human body, biological niches change drastically, including via interactions with surrounding cells and different energy sources. Ingestion of human cells has been proposed as a direct process that parasitic protozoa deploy as an inside-host survival mechanism. Therefore, the sensing of host nutrients is a potential target for inhibiting pathogenesis, which is an extensively studied subject in research to address parasite virulence [1].

Balamuthia mandrillaris is a natural nonsymbiotic amoeba that lives freely in soil and fresh water worldwide [2]. Despite being an environmental microorganism, *B. mandrillaris* is pathogenic to humans and can infect the brain, causing hemorrhagic necrosis known as granulomatous amoebic encephalitis (GAE) in the brain parenchyma. Although GAE is rare globally [3], it is a life-threatening disease in all age groups regardless of immune status [4]. The routes of transmission to humans include direct contact with soil via skin breakage or breathing dust or fresh water through the nose. The current treatment strategies vary and rely on a combination of antibiotic or antifungal drugs [5] [6] [7] [8]. Some regimens include drugs targeting *Leishmania* spp., a flagellate parasitic protozoan. Nevertheless, none of these strategies are effective, contributing to a high mortality rate (~ 98%) [9]. To date, only six patients have recovered after treatment with the following drug regimen: pentamidine isethionate, 5-flucytosine, fluconazole, and a macrolide (clarithromycin or azithromycin) with or without sulfadiazine, miltefosine,

thioridazine or liposomal amphotericin B [10]. However, these drug combinations require long-term application, ranging from approximately months to years. Given its extreme rarity and difficult diagnosis, GAE is a neglected parasitic disease with a high mortality rate.

Attempts to develop new drugs have focused primarily on inhibiting the survival of the *B. mandrillaris* trophozoite, the vegetative stage. To examine amoebicidal activity, human cell-free culture of *B. mandrillaris* trophozoites is useful for high-throughput drug screening. Given its ability to survive in the *in vivo* microenvironment, the use of human cell-free cultures does not allow the study of the process by which trophozoites acquire nutrients from the surrounding human cells. Studies have shown a cell contact-dependent mechanism in which *B. mandrillaris* trophozoites protrude into the cytoplasm to envelop and invade murine cells [11]. Dunnebacke proposed a cell-in-cell formation of *B. mandrillaris* trophozoites in African green monkey kidney cells, followed by human cell death [12]. Nevertheless, none of the studies demonstrated cellular uptake of human cells. Specifically, what cell components are ingested and in what form remain unaddressed. A recent study demonstrated that the epithelium-invading *Entamoeba histolytica* trophozoites nibbled parts of the human cell cytoplasm, a process defined as trogocytosis. However, trogocytosis by *B. mandrillaris* trophozoites has not been reported to date. Altogether, the mechanism by which the *B. mandrillaris* trophozoite utilizes human neuron-related cells as an energy source for survival remains uncertain.

To gain evidence of cellular uptake, this study used a confocal microscope and a holotomographic microscope for imaging cell-to-cell interactions in a three-dimensional (3D) manner. To mimic human neurons, a conventional culture of the human neuroblastoma SH-SY5Y cell line was performed. Ingestion of human cell components was monitored using fluorescent probes specific to lipids, proteins, and nucleic acids. Overall, we propose a trogocytosis-independent mechanism by which *B. mandrillaris* trophozoites take up cell components in standard 2D culture.

Methods

Culture of human neuroblastoma cells

The human neuroblastoma SH-SY5Y cell line (ATCC® No. CRL-2266™, VA) was cultured in a mixture of ATCC-formulated Eagle's minimum essential medium and F12 medium (1:1 ratio) supplemented with 10% fetal bovine serum, hereinafter called complete EMEM-F12. The culture was incubated at 37°C in a humidified atmosphere containing 5% CO₂. Subculture was performed when cells reached 60–80% confluence following the ATCC's instructions.

Coculture of *B. mandrillaris* trophozoites with human neuroblastoma cells

B. mandrillaris trophozoites were cultured with human neuroblastoma SH-SY5Y cells using medium and conditions similar to those used for the culture of human neuroblastoma cells. Subculture of the amoeba was performed when more than 90% of human neuroblastoma cells disappeared but prior to the formation of cysts (less than 5% to enrich trophozoites). The floating trophozoites were collected and diluted with complete EMEM-F12 medium at a ratio of 1:5, followed by plating into a cell culture well containing human neuroblastoma cells at 80% confluence.

Cell labeling with fluorescent probes

SH-SY5Y cells were cultured at a density of 2.5×10^5 cells/250 μ L in a well of a 48-well polystyrene plastic plate. At 72 hours postculture, the medium was removed, and the cells were washed once with PBS. To label amines, Cell Tracker™ Green CMFDA (Invitrogen, OR) prepared at 2.5 μ M in complete EMEM/F12 medium was incubated with the cells for 45 min at 37°C in a 5% CO₂ incubator. For lipid binding, Vybrant™ DiD Cell-Labeling Solution (Invitrogen, OR) was prepared at a 1:1600 dilution in complete EMEM-F12 medium for 15 min as mentioned above. After labeling, the cells were washed 2–3 times with PBS to remove excess probes. Culture of SH-SY5Y cells labeled with *B. mandrillaris* trophozoites was performed within 3 hours post cell labeling.

Confocal imaging of fluorescently labeled cells

To visualize cell–cell interactions in a snapshot manner, human neuroblastoma SH-SY5Y cells were allowed to adhere to a glass plate inserted into a well of a cell culture plate. At each time point, the culture medium was removed, and the cells were fixed with 2% paraformaldehyde in PBS for 30 min at 37°C. The glass plate was lifted and placed upside down on a glass microscope slide. A drop of Fluoroshield Mounting Medium with DAPI (Abcam) was used for mounting the glass plate with adherent cells on the glass microscope slide. The cell-mounted microscope slides were kept in the dark prior to visualization under a confocal microscope (Nikon A1R, Japan). For floating cells, the culture medium was harvested and centrifuged at 1,200 rpm for 5 min at room temperature. After removal of the culture medium, the cell pellet was dispersed in polyvinyl alcohol as a fixative agent. A total of 20–25 μ L of cell suspension was dropped and smeared on a glass microscope slide by circling the plastic tip in an outward direction. After air drying in the dark, the cell-mounted slide was subjected to microscopic imaging as mentioned above.

Three-dimensional imaging

To observe cell-to-cell interactions in a 3D manner, cocultures of *B. mandrillaris* trophozoites with human SH-SY5Y cells were subjected to visualization under a holotomographic microscope (Tomocube, South Korea). When a light beam traverses a cell, each cellular compartment scatters light differently, generating an optical parameter known as the reflective index (RI). Hence, cells can be visualized based on the RI of the cellular compartments, allowing fluorescence-free imaging. Moreover, 360-degree rotation of the light source allows the construction of a holographic image of cell-to-cell interactions. Human neuroblastoma SH-SY5Y cells were cultured in a cell culture dish in a centered quadrilateral well (TomoDish, Daejeon, South Korea). The trophozoites were placed in the wells and subjected to 3D

imaging. In some experiments, fluorescent probes were used to image the ingestion of human cells in a real-time manner.

Inhibition of trogocytosis

Wortmannin (Sigma-Aldrich, MO), a phosphatidylinositol-3 kinase inhibitor, was incubated with the trophozoites following a previous report [13]. After removing the inhibitors, the trophozoites were cocultured with human neuroblastoma cells attached to a glass plate. Cells were observed using a confocal microscope as mentioned above.

Cytotoxicity assays

Loss of cell membrane integrity was examined using trypan blue (ThermoFisher), a conventional visible dye, and SYTOX™ Blue Dead Cell Stain (Molecular probe, OR, USA). For trypan blue staining, the culture medium was removed, and 0.4% trypan blue-containing PBS was added. After 1–2 min of incubation, the cells were washed with PBS and observed under an inverted microscope. For SYTOX Blue staining, human SH-SY5Y cells were plated on a glass slide placed in a well of a cell culture plate. After incubation with *B. mandrillaris* trophozoites, SYTOX Blue was added to the culture medium for 5 min, and the cells were fixed to the glass using 4% PFA in PBS and mounted with an antifade medium (Fluoroshield Mounting Medium with DAPI, Abcam). To distinguish trophozoites and human cells, differential interference contrast or CMFDA labeling was used to identify the cell shape of *B. mandrillaris* trophozoites. Cells were observed using a confocal microscope (Nikon AIR, Japan).

Quantitative PCR

Human neuroblastoma SH-SY5Y cells were subjected to RNA extraction using FavorPrep™ Tissue Total RNA Extraction Mini Kit (Favorgen, Ping-Tung, Taiwan). The concentration and purity of the RNA were examined using a Nanodrop (Thermo Scientific). The threshold for RNA purity was higher than 1.80. The mRNA was reverse transcribed to cDNA using the oligo-dT primer of iScript™ Reverse Transcription Supermix (Bio-Rad, Hercules, CA, USA). The cDNA was used as a template to amplify B-cell lymphoma 2 (*BCL2*) and BCL2 associated X (*BAX*) transcripts. PCR was performed using Luna® Universal qPCR Master Mix (New England Biolabs), consisting of a forward primer (5'-TCATGTGTGTGGAGAGCGTC-3') and reverse primer (5'-TCAGTCATCCACAGGGCGAT-3') for the *BCL2* transcript [14] and a forward primer (5'-TCAGGATGCGTCCACCAAGAAG-3') and reverse primer (5'-TGTGTCCACGGCGGCAATCATC-3') for the *BAX* transcript [15]. Following a 3-min denaturation at 95°C, DNA amplification included 40 rounds of denaturation at 95°C for 15 seconds and annealing-extension at 60°C for 30 seconds. The level of the human *ACTB* transcript was set as an internal control to normalize the levels of *BCL2* and *BAX* transcripts among samples. Threshold cycles of the samples were subjected to a calculation of relative gene expression based on the $2^{-\Delta\Delta CT}$ method [16].

Statistical analysis

The mean and standard deviation were calculated from at least three independent experiments. Graph plotting and statistical analysis were performed using GraphPad Prism 7. Student's t test was used to

compare the means of two different experimental settings, and a *p* value of less than 0.05 was regarded as statistically significant.

Results

In 2D culture, human neuroblastoma SH-SY5Y cells exhibit a neuroblast-like morphology with a few short neurite-like projections (arrowheads in the right panel of Fig. 1A). At 70–80% confluence, the trophozoites of *B. mandrillaris* were added to the culture medium of human neuroblastoma cells and plated on a monolayer of human neuroblastoma SH-SY5Y cells. Within 30 min, nearly all of the trophozoites became attached to the human cells. At 24 hours post coculture, a human cell-free area appeared and increased in size in a time-dependent manner (the dotted line in Fig. 1B). At higher magnification, there were round cells at the edge of the human cell-free zone (arrowheads in inset #1 in the right panel of Fig. 1B and the left panel of Fig. 1C), while the irregularly shaped, cytoplasm-protruding trophozoites were located at the center of the human cell-free area (arrow in inset #2 in the right panel of Fig. 1B and the right panel of Fig. 1C). Live imaging of the inverted phase contrast microscope shows a trophozoite attached to human cells and protruding pseudopods. The human cell-adhering trophozoite also rotated, while its pseudopods occasionally elongated and shortened (Additional file 1).

To examine the cytotoxicity of the *B. mandrillaris* trophozoites, live cell-impermeable trypan blue dye was added at 24 hours post coculture. The trypan blue-positive human neuroblastoma cells were proximal to the round trophozoites (inset #1–3 in Fig. 1D), indicating cell death due to loss of cell membrane integrity. In contrast, the trophozoite-free human cells were viable (inset #4 in the right panel of Fig. 1D). Downregulation of anti-apoptotic *BCL2* transcripts were observed at one hour post coculture, while levels of apoptotic *BAX* transcripts tended to be upregulated but not significant difference (Fig. 1E). After 2 days, the monolayer of human neuroblastoma cells was entirely destroyed (upper panel of Fig. 1F). Cell debris, pseudopod-protruding trophozoites and floating round shaped cells were scattered throughout the culture well (insets#1–4, Fig. 1F). Together, the findings showed that the clinically isolated *B. mandrillaris* trophozoites were cytotoxic to human neuroblastoma SH-SY5Y cells.

To observe the mechanism by which the trophozoites ingest human cellular components in real time, a holotomographic microscope was used to capture 360-degree views of the 2D-cultured cells (Fig. 2A). The 2D view of cells in the X-Y plane showed a difference in intensity from high to low (white to black, Fig. S1). The dense white-colored circles observed in the 2D image of human cells were lipid droplet-like structures (arrowhead in Fig. S1). Based on morphology, the white oval shape was distinct from the elongated shape with protruding pseudopods. However, without the cell morphology, it was difficult to distinguish between the human cells and trophozoites in the 2D image (Fig. S1A).

Given that different types of cell components exhibit distinct RIs, the holotomographic microscope is capable of visualizing cell components in a 3D manner. Based on the RIs of the cell components, pseudocolors were assigned for each cell component. As shown in the X-Y plane (left panel in Fig. 2B), the cytoplasm of human neuronal cells exhibited a cyan color, while that of trophozoites displayed a blue

gray color. The red dots that had an RI similar to that of the lipid droplets were observed along the X-Y, X-Z and Y-Z planes (arrowheads in all panels of Fig. 2B and Additional file 2). For the second representative cell image, the X-Y plane showed oval-shaped cells with a protruding pseudopod-like structure. When observing the lateral view along the Y-Z planes, there was a bridge between the human neuroblastoma cells and *B. mandrillaris* trophozoites (arrows in the middle and left panels of Fig. 2C and Additional file 3). Thus, the difference in the RI between human neuroblastoma cells and *B. mandrillaris* trophozoites allows the identification of the cell type and connecting point.

To observe the movement of the trophozoites, live imaging was performed using holotomography to observe cell-to-cell interactions. The 3D live imaging revealed that the *B. mandrillaris* trophozoite twisted its extending pseudopod (Additional file 4). When trophozoite rotation was imaged for 6 seconds, the snapshot image shows anchoring sites (arrows in the left, middle and right panels of Fig. 2D). Notably, the number of cyan-colored components increased in the pseudopod-protruding trophozoite when observed for 6 seconds (arrowhead in the middle and right panels of Fig. 2D). Taken together, the results showed that the *B. mandrillaris* trophozoite anchors to the human cell, followed by twisting its extending cytoplasm around the cytoplasmic bridge.

Given the similarity between the RIs of the human cells and the parasite, it was difficult to observe the invasion of the *B. mandrillaris* trophozoites. Thus, differential cell tracking was performed to observe a cell-to-cell interaction. Two fluorescence probes, CMFDA and DiD, were used to label amines and lipids, respectively (Fig. 3A). For human neuroblastoma SH-SY5Y cells, CMFDA was observed as a smear pattern dispersed throughout the cytoplasm, while DiD was observed as a granule-like pattern in the cytoplasm and on the cell membrane (Fig. S2A). In contrast, the cytoplasm of *B. mandrillaris* trophozoites exhibited a dispersed pattern of DiD-labeled lipids. There was no cellular component labeled with CMFDA (Fig. S2B). Hence, the CMFDA and DiD fluorescent probes were used for tracking human neuroblastoma cells and *B. mandrillaris* trophozoites, respectively (Fig. S2C).

Based on light microscopic observation, the whole trophozoites reportedly entered African green monkey kidney cells [12]. To confirm the cell-in-cell formation, CMFDA and DiD were used to label the respective human cells and the *B. mandrillaris* trophozoites to detect human cell-invading *B. mandrillaris* trophozoites (Fig. 3A). After 40 min of coculture on a glass slide, the X-Y plane of the 2D-captured image showed DiD-labeled *B. mandrillaris* trophozoites (magenta, Fig. 3B) located proximal to the CMFDA-labeled human neuronal cells (green, in Fig. 3B). The trophozoites were positioned at the top of human neuroblastoma cells. Some trophozoites were partially adhered to the human cells (insets 1 and 3 of Fig. 3B), while some spread their cytoplasm across a few human cells (inlet 2 of Fig. 3B). There were no yellow-colored merged areas, suggesting that none of the trophozoites entered the human cells.

To observe the invasion by *B. mandrillaris* trophozoites into human neuroblastoma cells, differential cell tracking was performed as mentioned above (Fig. 3A). At 40 min post coculture, magenta-colored holes were observed in the cytoplasm of human cells (arrows in all panels of Fig. 3C), indicating the presence of DiD-labeled lipids in *B. mandrillaris* trophozoites. By using the Z-stack, the X-Z and Y-Z planes allow a

lateral view of the imaged cells (left panel of Fig. 1C). Thus, both the X-Z and Y-Z planes revealed that the DiD-labeled compartment was surrounded by the human cytoplasm (green) and was proximal to the human nucleus (left panel of Fig. 3C). Around the cytoplasmic hole, the intensity of CMFDA fluorescence was higher than that in other parts of the human cytoplasm (arrowheads in the middle panel of Fig. 3D). The lipid-containing cytoplasm of the *B. mandrillaris* trophozoite protruded into human cells, a structure mimicking invadopodia (yellow arrows in the right panel of Fig. 3C). A 3-D view of the X-Y-Z plane shows the invadopodia-like structure of *B. mandrillaris* trophozoites protruding into human neuroblastoma cells (yellow arrow in Fig. 3D and Additional file 5).

Following invasion, the cellular uptake of the *B. mandrillaris* trophozoites was examined. To observe components of human cells inside the trophozoites, both CMFDA and DiD fluorescence probes were preincubated with human neuroblastoma cells, while the *B. mandrillaris* trophozoites remained unstained (Fig. 3E). In the cytoplasm of the *B. mandrillaris* trophozoites (dotted line in Fig. 3F), the amine-containing cell components appeared as well-defined granules with irregular sizes. In contrast, the lipid components were nonuniformly dispersed throughout the cytoplasm of *B. mandrillaris* trophozoites (Fig. 3F). The pattern of human-derived lipids in the cytoplasm of the trophozoites was similar to that of *B. mandrillaris*-derived lipids (Fig. S2B). The majority of amines and lipids showed no overlap, indicating the existence of a distinct cellular compartment (merge panel of Fig. 3F). Moreover, the trophozoite contained sparse granular nuclei with smaller sizes than human nuclei (arrowheads in Fig. 3F). When the cellular uptake was examined, the percentages of CMFDA- and DiD-positive trophozoites adhering to human cells increased to 96% at 40 min post coculture (Fig. 3G). However, there were no changes in the proportion of human cell-ingesting floating trophozoites from 10–40 min. However, after 6 hours of coculture, the *B. mandrillaris* trophozoites were mostly detached and floated in the culture medium. The floating trophozoites had ingested the human cell components, which appeared as amine-containing, irregularly shaped granules and lipid-diffused areas in the trophozoite cytoplasm (Fig. S3). Altogether, these results suggest that the *B. mandrillaris* trophozoite protrudes its cytoplasm into human cells, forming a structure mimicking invadopodia, prior to ingesting human cell components.

To visualize ingestion of the human cell cytoplasm in real time, the human cells were cultured as a 2D monolayer and incubated with the amine-binding fluorescent dye CMFDA (Fig. 4A). The nonlabeled trophozoites were cocultured with CMFDA-labeled human cells. At 6 hours post coculture, sparse green circular shapes were observed in the cytoplasm of the trophozoites. Live imaging showed that green vesicles appeared in the area proximal to the human cells (Additional file 6). Within 13 min, the colored area in the human cytoplasm increased, suggesting loss of the cytoplasmic compartment (inlets in Fig. 4B). Subsequently, the human cells lost cell membrane integrity, likely due to apoptosis (Fig. 4C). Thus, the *B. mandrillaris* trophozoites ingested the human protein constituent in the form of spherical granules, a finding similar to the 2D snapshot confocal images in Fig. 3F.

The phosphatidylinositol-3 kinase (PI3K) pathway plays an important role in trogocytosis, a process in which parasitic amoebae ingest portions of human cells [13]. To investigate whether human cell ingestion by *B. mandrillaris* relies on the PI3K signal, human trophozoites were preincubated with

wortmannin, a PI3K inhibitor, prior to 40-min coculture with CMFDA-labeled human cells (Fig. 4C). Number of the CMFDA- and DiD-positive trophozoites indicated that the *B. mandrillaris* trophozoites incubated with wortmannin retained the capability of ingesting human amine-containing components, indicating that ingestion by *B. mandrillaris* trophozoites was trogocytosis independent (Fig. 4D).

Discussion

In this study, the mechanism underlying *B. mandrillaris*-induced cellular damage was examined in a standard 2D culture of human neuroblastoma cells. Based on the 3D live imaging results, the anchoring-to-twisting behavior of the *B. mandrillaris* trophozoites was proposed. The 3D view of the confocal images revealed that the invadopodia first penetrate human cells. Subsequently, the trophozoites ingest human cell contents in two different forms: (1) protein-containing, nonmembranous droplets and (2) lipid-dispersed patterns. Inhibition of cell nibbling or trogocytosis failed to suppress these processes. Thus, the mechanism of cytopathogenicity of *B. mandrillaris* trophozoites is likely different from trogocytosis.

Despite the long-known effects on host cell death [17], the cellular uptake of pathogenic *B. mandrillaris* remains largely unaddressed. The number of studies conducted on the cytopathogenicity of *B. mandrillaris* to date is limited [11] [12]. Kiderlen used murine mastocytoma P815 cells, an adherent phagocytic cell line derived from mast cells, to study the cytopathogenicity of a mandrill baboon-derived *B. mandrillaris* isolate [11]. Based on scanning electron microscopy and transmission electron microscopy, engulfment and cytoplasmic protrusion of *B. mandrillaris* trophozoites were observed, leading to murine cell lysis. Hence, the cytopathogenicity of *B. mandrillaris* has been attributed to phagocytosis. Based on phase contrast images, Dunnebacke reported that *B. mandrillaris* entered the cytoplasm of African green monkey kidney cells [12]. Overall, 2D cultures of mouse and monkey-derived cells allowed observation of cell-to-cell interactions mainly in a 2D manner.

Similar to previous studies, the current study used the 3D view of a confocal image for visualizing invadopodia. However, the 3D confocal images did not show internalization of the *B. mandrillaris* trophozoite into human cells, a cell-in-cell formation process [12]. The discrepancy may result from the host cell types, amoeba strains and observation methods. Nevertheless, the use of a confocal microscope is more practical for laboratories equipped with a 3D fluorescence microscope. Advances in high-resolution imaging may support quantitative analysis of confocal images, preventing subjective interpretation. Moreover, live microscopic observation showed the position of the *B. mandrillaris* trophozoite on the top or beside human neuroblastoma cells during cellular uptake. However, the holotomographic imaging in the current study had limitations. First, the experiment was performed in a short period of 3 hours due to the lack of a CO₂ incubator with the holotomographic microscope. Second, the fluorescence intensity of CMFDA was diminished after light exposure, a process known as photobleaching. Thus, cell tracking with a more light-resistant fluorescent dye in a closed system will allow long-term observation under physiologically relevant conditions in real time.

Trogocytosis is the process by which parts of the target cell membrane are cut and internalized and was first demonstrated in *Naegleria fowleri*, a parasitic amoeba causing GAE [19]. Immune cells use trogocytosis for cell–cell communication, in which the nibbling immune cells display membranous proteins of other immune cells to trigger defensive mechanisms [20] [21] [22] [23]. Moreover, neutrophils also use trogocytosis to kill cancer cells and the urogenital tract-dwelling *Trichomonas vaginalis*. On the other hand, *E. histolytica* trophozoites, which are obligate parasitic amoebae, reportedly use trogocytosis to acquire the lipid-membrane-bound protein of human Jurkat T cells [13]. In addition to being an energy source, *E. histolytica* trophozoites display human membranous protein to be disguised from host immune cells [24], a process known as cross-dressing. Whether *B. mandrillaris* trophozoites utilize human membrane proteins to escape the innate immune defense of the host needs to be further investigated.

The data in this study indicate the trogocytosis-independent process to be a way to gain nutrients from human cells. Nevertheless, the reliability of some supporting evidence and limitations of the methods used should be considered. By using protein- and lipid-binding fluorescent dyes for 3D confocal microscopy, the *B. mandrillaris* trophozoites were found to take up human proteins in vesicle-like structures but lacked a phospholipid membrane. Thus, the process by which parts of ingested target cells are surrounded by phospholipid membranes is unlikely to be endocytosis or trogocytosis. In contrast, the human lipid components dispersed nonuniformly throughout the cytoplasm of the *B. mandrillaris* trophozoites, indicating the different ways for the transfer of lipids and proteins. Second, Rolstone and colleagues clearly demonstrated that *E. histolytica* trophozoites take up lipid membrane-bound protein-containing vesicles from human leukemic T cells. Pretreatment with the PI3K inhibitor wortmannin suppressed the trogocytosis of *E. histolytica*. In contrast, interruption of the PI3K signal failed to inhibit the cellular uptake of *B. mandrillaris* trophozoites. Notably, the use of adherent and floating human cells to demonstrate cellular uptake may result in different interpretations of cellular uptake. Floating cancer cells take up particles in a phagocytosis-like manner at levels higher than that observed with adherent cancer cells [25]. Thus, an investigation of cellular uptake should be performed in a more physiologically relevant setting, i.e., cerebral organoid, neural spheroid or *ex vivo* culture of human brain tissue [26].

CMFDA and DiD are fluorescent dyes that bind to amines and lipids, respectively. Human neuroblastoma cells exhibited a CMFDA-labeled cytoplasm, which contained protein, and a DiD-labeled phospholipid bilayer of the cell membrane. Moreover, labeling of the *B. mandrillaris* trophozoites using CMFDA and DiD showed a similar pattern to that of human neuroblastoma cells: CMFDA in the cytoplasm and DiD on the cell membrane. Therefore, the use of both cell tracking dyes is a reliable method to track cell components. However, there were limitations to 3D imaging in this study. Confocal microscopy allows laser-based 3D imaging of cells in a fixed form at a certain time point. Given the dynamic process of cellular uptake, live imaging would allow observation of cell physiological phenomena in a relatively real-time manner. Thus, a holotomographic microscope was used to observe cellular uptake. However, the holotomographic microscope used in this study allowed only visualization of CMFDA.

To confirm the presence of invadopodia and occurrence of endocytosis, additional experiments in which these processes are inhibited using small-molecule inhibitors are needed. Wortmannin, an inhibitor of the

PI3K signaling pathway, was able to inhibit amoebic trophocytosis of *E. histolytica* trophozoites despite a lack of data supporting defects in PI3K signaling. Moreover, wortmannin-mediated PI3K inhibition of *Dictyostelium discoideum*, a single- or multiple-cell organism in the phylum amoebozoa, decreased the formation of bacteria-containing phagosomes. Thus, actin polymerization-mediated trophocytosis is an unlikely mechanism used by *B. mandrillaris*. To our knowledge, there are no assays to validate the effectiveness of PI3K inhibition in the trophozoites of *B. mandrillaris*, limiting the assessment of wortmannin's effect in our experiments. Nevertheless, pretreating *B. mandrillaris* trophozoites with wortmannin did not inhibit cellular uptake.

B. mandrillaris trophozoites have been cocultured with feeder cells derived from human or nonhuman origin. African green monkey kidney cells, also known as Vero cells, supported the growth of *B. mandrillaris* isolated from the autopsied brain of a pregnant baboon (*Papio sphinx*) that died from meningoencephalitis, whereas human lung carcinoma MRC-5 cells failed to do so [18]. To our knowledge, human lung carcinoma A549 cells supported the growth of *B. mandrillaris* isolated from the autopsied brain of a Thai patient. In contrast, the use of human neuroblastoma SH-SY5Y cells showed that Thai *Acanthamoeba* isolate caused human cell death via downregulation of apoptotic *BAX* gene expression. In this view, the trophozoites ingest and damage these cells regardless of the type, leading to cell death and removal of host cells from culture. Despite severe damage to feeder cells, the mechanisms of cytopathogenicity have not been investigated.

Given the physiological relevance to mature neurons, the human neuroblastoma SH-SY5Y cell line was used as a model for studies of neurotropic pathogens, neurodegenerative disease and neuronal differentiation. Most fatal clinical manifestations of Balamuthia encephalitis are caused by neuropathogenesis, including cell death in the brain parenchyma. Thus, SH-SY5Y is more relevant to human physiology than other cell lines. Notably, human SH-SY5Y cells can be induced to differentiate into mature neurons [27], allowing the screening of cytotoxicity in a high-throughput manner with more physiological relevance than undifferentiated cells [28].

Although the conventional 2D culture of human cancer cell lines is useful for studying host-parasite interactions, the current *in vitro* models have gradually shifted to a more physiologically relevant 3D setting. Spheroids and organoids are 3D culture systems in which cells are organized in a cluster, allowing intercellular interactions in all dimensions and gradient exposure to external stimuli. The 2D-cultured cells differ from those of the 3D culture, including equal exposure to nutrients and gas, cell-cell interactions, and cell-rigid surface interactions. As a result, several biological processes of cells were not similar between the 2D and 3D results. Spheroids of human neuroblastoma SH-SY5Y cells were relatively more mature than the 2D cell culture [29]. Therefore, the use of spheroids may address the gap in our understanding of the cytopathogenicity of *B. mandrillaris*.

Conclusion

A clinical isolate of *B. mandrillaris* trophozoites is cytotoxic to human neuroblastoma SH-SY5Y cells. The 3D imaging revealed the anchoring-to-twisting behavior of the *B. mandrillaris* trophozoites. The addition of a Z-plane during confocal observation allowed visualization of invadopodia penetrating the human cytoplasm. There were at least two different types of cellular uptake: protein-containing, nonmembranous, well-defined granules and dispersed smears of lipid components. Inhibition of PI3K-mediated trogocytosis failed to suppress the cellular uptake of *B. mandrillaris* trophozoites, suggesting the existence of trogocytosis-independent cytopathogenicity.

Abbreviations

BAX: BCL2-associated X; BCL2: B-cell lymphoma 2; CMFDA: 5-chloromethylfluorescein diacetate; DiD: 1,1-dioctadecyl-3,3,3,3-tetramethylindodicarbocyanine; EMEM: Eagle's minimum essential medium; GAE: granulomatous amoebic encephalitis; PBS: phosphate-buffered saline; PI3K, phosphoinositide 3-kinase; qPCR: quantitative polymerase chain reaction

Declarations

Acknowledgments

We would like to thank all staff at the Department of Parasitology, Faculty of Medicine Siriraj Hospital, for technical advice. The technical assistance provided by Miss Bongkotchakorn Peereeyaphat and Miss Arisasa Issarachaiwong, the staff member at Hollywood International Ltd., Thailand, in the use of Tomocube is greatly appreciated.

Funding

This research project was supported partly by the Faculty of Medicine Siriraj Hospital, Mahidol University. P.W. is supported by the Siriraj Graduate Scholarship, Faculty of Medicine Siriraj Hospital, Mahidol University. K.K. is supported by the Research Career Development Grant of the Thailand Science Research and Innovation and Mahidol University (grant number RSA6280102) and a grant for Mid-career Talented Researchers provided by the National Council of Thailand.

Availability of data and materials

All data generated or analyzed during this study are included in this published article and its Additional information files.

Authors' contributions

KK designed the scope of the study and wrote the manuscript.

WP designed and performed the experiments and wrote the manuscript.

PTS designed and performed experiments.

NT performed experiments.

NW performed experiments.

Ethics approval and consent to participate

The *B. mandrillaris* trophozoites were clinically isolated from a human subject with consent to participate (COA no. Si806/2020). For all experiments in this study, the use of *B. mandrillaris* trophozoites received ethics approval (COA. no. 146/2022).

Consent for publication

All authors have given consent for publication.

Competing interests

The authors declare that they have no conflicts of interest.

Corresponding author contact information

Assistant Prof. Kasem Kulkeaw, PhD

Siriraj Integrative Center for Neglected Parasitic Diseases (SiCNPd)

Department of Parasitology, Faculty of Medicine Siriraj Hospital, Mahidol University

7th floor Adulyadejvikrom Building, 2 Wang Lang Road, Khwaeng Siriraj, Khet Bangkok-noi, Bangkok 10700, Thailand

Tel: 02-419-6468 ext. 96484, e-mail address: kasem.kuk@mahidol.edu

References

1. Zuzarte-Luis V, Mota MM. Parasite Sensing of Host Nutrients and Environmental Cues. *Cell Host Microbe*. 2018;23 6:749 – 58; doi: 10.1016/j.chom.2018.05.018. <https://www.ncbi.nlm.nih.gov/pubmed/29902440>.
2. Piper KJ, Foster H, Susanto D, Maree CL, Thornton SD, Cobbs CS. Fatal Balamuthia mandrillaris brain infection associated with improper nasal lavage. *Int J Infect Dis*. 2018;77:18–22; doi: 10.1016/j.ijid.2018.09.013. <https://www.ncbi.nlm.nih.gov/pubmed/30243910>.
3. Cope JR, Landa J, Nethercut H, Collier SA, Glaser C, Moser M, et al. The Epidemiology and Clinical Features of Balamuthia mandrillaris Disease in the United States, 1974–2016. *Clin Infect Dis*. 2019;68 11:1815–22; doi: 10.1093/cid/ciy813. <https://www.ncbi.nlm.nih.gov/pubmed/30239654>.

4. Gompf SG, Garcia C. Lethal encounters: The evolving spectrum of amoebic meningoencephalitis. *IDCases*. 2019;15:e00524; doi: 10.1016/j.idcr.2019.e00524.
<https://www.ncbi.nlm.nih.gov/pubmed/30937287>.
5. Cary LC, Maul E, Potter C, Wong P, Nelson PT, Given C, 2nd, et al. Balamuthia mandrillaris meningoencephalitis: survival of a pediatric patient. *Pediatrics*. 2010;125 3:e699-703; doi: 10.1542/peds.2009-1797. <https://www.ncbi.nlm.nih.gov/pubmed/20123772>.
6. Martinez DY, Seas C, Bravo F, Legua P, Ramos C, Cabello AM, et al. Successful treatment of Balamuthia mandrillaris amoebic infection with extensive neurological and cutaneous involvement. *Clin Infect Dis*. 2010;51 2:e7-11; doi: 10.1086/653609.
<https://www.ncbi.nlm.nih.gov/pubmed/20550438>.
7. Doyle JS, Campbell E, Fuller A, Spelman DW, Cameron R, Malham G, et al. Balamuthia mandrillaris brain abscess successfully treated with complete surgical excision and prolonged combination antimicrobial therapy. *J Neurosurg*. 2011;114 2:458–62; doi: 10.3171/2010.10.JNS10677.
<https://www.ncbi.nlm.nih.gov/pubmed/21073255>.
8. Orozco L, Hanigan W, Khan M, Fratkin J, Lee M. Neurosurgical intervention in the diagnosis and treatment of Balamuthia mandrillaris encephalitis. *J Neurosurg*. 2011;115 3:636 – 40; doi: 10.3171/2011.4.JNS102057. <https://www.ncbi.nlm.nih.gov/pubmed/21619411>.
9. Siddiqui R, Matin A, Warhurst D, Stins M, Khan NA. Effect of antimicrobial compounds on Balamuthia mandrillaris encystment and human brain microvascular endothelial cell cytopathogenicity. *Antimicrob Agents Chemother*. 2007;51 12:4471–3; doi: 10.1128/AAC.00373-07.
<https://www.ncbi.nlm.nih.gov/pubmed/17875991>.
10. Bravo FG, Seas C. Balamuthia mandrillaris amoebic encephalitis: an emerging parasitic infection. *Curr Infect Dis Rep*. 2012;14 4:391–6; doi: 10.1007/s11908-012-0266-4.
<https://www.ncbi.nlm.nih.gov/pubmed/22729402>.
11. Kiderlen AF, Tata PS, Ozel M, Laube U, Radam E, Schafer H. Cytopathogenicity of Balamuthia mandrillaris, an opportunistic causative agent of granulomatous amebic encephalitis. *J Eukaryot Microbiol*. 2006;53 6:456–63; doi: 10.1111/j.1550-7408.2006.00130.x.
<https://www.ncbi.nlm.nih.gov/pubmed/17123409>.
12. Dunnebacke TH. The ameba Balamuthia mandrillaris feeds by entering into mammalian cells in culture. *J Eukaryot Microbiol*. 2007;54 5:452–64; doi: 10.1111/j.1550-7408.2007.00286.x.
<https://www.ncbi.nlm.nih.gov/pubmed/17910691>.
13. Ralston KS, Solga MD, Mackey-Lawrence NM, Somlata, Bhattacharya A, Petri WA, Jr. Trophocytosis by Entamoeba histolytica contributes to cell killing and tissue invasion. *Nature*. 2014;508 7497:526–30; doi: 10.1038/nature13242. <https://www.ncbi.nlm.nih.gov/pubmed/24717428>.
14. Almeida AS, Soares NL, Vieira M, Gramsbergen JB, Vieira HL. Carbon Monoxide Releasing Molecule-A1 (CORM-A1) Improves Neurogenesis: Increase of Neuronal Differentiation Yield by Preventing Cell Death. *PLoS One*. 2016;11 5:e0154781; doi: 10.1371/journal.pone.0154781.
<https://www.ncbi.nlm.nih.gov/pubmed/27144388>.

15. Roh JI, Lee J, Sung YH, Oh J, Hyeon DY, Kim Y, et al. Impaired AKT signaling and lung tumorigenesis by PIERCE1 ablation in KRAS-mutant non-small cell lung cancer. *Oncogene*. 2020;39 36:5876–87; doi: 10.1038/s41388-020-01399-5. <https://www.ncbi.nlm.nih.gov/pubmed/32728173>.
16. Rao X, Huang X, Zhou Z, Lin X. An improvement of the 2^{ΔΔCT} method for quantitative real-time polymerase chain reaction data analysis. *Biostat Bioinforma Biomath*. 2013;3 3:71–85. <https://www.ncbi.nlm.nih.gov/pubmed/25558171>.
17. Guarner J, Bartlett J, Shieh WJ, Paddock CD, Visvesvara GS, Zaki SR. Histopathologic spectrum and immunohistochemical diagnosis of amebic meningoencephalitis. *Mod Pathol*. 2007;20 12:1230–7; doi: 10.1038/modpathol.3800973. <https://www.ncbi.nlm.nih.gov/pubmed/17932496>.
18. Visvesvara GS, Martinez AJ, Schuster FL, Leitch GJ, Wallace SV, Sawyer TK, et al. Leptomyxid ameba, a new agent of amebic meningoencephalitis in humans and animals. *J Clin Microbiol*. 1990;28 12:2750–6; doi: 10.1128/jcm.28.12.2750-2756.1990. <https://www.ncbi.nlm.nih.gov/pubmed/2280005>.
19. Brown T. Observations by immunofluorescence microscopy and electron microscopy on the cytopathogenicity of *Naegleria fowleri* in mouse embryo-cell cultures. *J Med Microbiol*. 1979;12 3:363–71; doi: 10.1099/00222615-12-3-363. <https://www.ncbi.nlm.nih.gov/pubmed/381667>.
20. Sokol CL, Chu NQ, Yu S, Nish SA, Laufer TM, Medzhitov R. Basophils function as antigen-presenting cells for an allergen-induced T helper type 2 response. *Nat Immunol*. 2009;10 7:713–20; doi: 10.1038/ni.1738. <https://www.ncbi.nlm.nih.gov/pubmed/19465907>.
21. Perrigoue JG, Saenz SA, Siracusa MC, Allenspach EJ, Taylor BC, Giacomini PR, et al. MHC class II-dependent basophil-CD4 + T cell interactions promote T(H)2 cytokine-dependent immunity. *Nat Immunol*. 2009;10 7:697–705; doi: 10.1038/ni.1740. <https://www.ncbi.nlm.nih.gov/pubmed/19465906>.
22. Otsuka A, Nakajima S, Kubo M, Egawa G, Honda T, Kitoh A, et al. Basophils are required for the induction of Th2 immunity to haptens and peptide antigens. *Nat Commun*. 2013;4:1739; doi: 10.1038/ncomms2740. <https://www.ncbi.nlm.nih.gov/pubmed/23612279>.
23. Miyake K, Shiozawa N, Nagao T, Yoshikawa S, Yamanishi Y, Karasuyama H. Trogocytosis of peptide-MHC class II complexes from dendritic cells confers antigen-presenting ability on basophils. *Proc Natl Acad Sci U S A*. 2017;114 5:1111–6; doi: 10.1073/pnas.1615973114. <https://www.ncbi.nlm.nih.gov/pubmed/28096423>.
24. Miller HW, Suleiman RL, Ralston KS. Trogocytosis by *Entamoeba histolytica* Mediates Acquisition and Display of Human Cell Membrane Proteins and Evasion of Lysis by Human Serum. *mBio*. 2019;10 2; doi: 10.1128/mBio.00068-19. <https://www.ncbi.nlm.nih.gov/pubmed/31040235>.
25. Goldstein Y, Tischenko K, Brill-Karniely Y, Benny O. Enhanced Biomechanically Mediated "Phagocytosis" in Detached Tumor Cells. *Biomedicines*. 2021;9 8; doi: 10.3390/biomedicines9080947. <https://www.ncbi.nlm.nih.gov/pubmed/34440151>.
26. Lovett ML, Nieland TJF, Dingle YL, Kaplan DL. Innovations in 3-Dimensional Tissue Models of Human Brain Physiology and Diseases. *Adv Funct Mater*. 2020;30 44; doi:

- 10.1002/adfm.201909146. <https://www.ncbi.nlm.nih.gov/pubmed/34211358>.
27. Shipley MM, Mangold CA, Kuny CV, Szpara ML. Differentiated Human SH-SY5Y Cells Provide a Reductionist Model of Herpes Simplex Virus 1 Neurotropism. *J Virol.* 2017;91 23; doi: 10.1128/JVI.00958-17. <https://www.ncbi.nlm.nih.gov/pubmed/28956768>.
28. Dravid A, Raos B, Svirskis D, O'Carroll SJ. Optimised techniques for high-throughput screening of differentiated SH-SY5Y cells and application for neurite outgrowth assays. *Sci Rep.* 2021;11 1:23935; doi: 10.1038/s41598-021-03442-1. <https://www.ncbi.nlm.nih.gov/pubmed/34907283>.
29. Jung GS, Lee KM, Park JK, Choi SK, Jeon WB. Morphogenetic and neuronal characterization of human neuroblastoma multicellular spheroids cultured under undifferentiated and all-trans-retinoic acid-differentiated conditions. *BMB Rep.* 2013;46 5:276–81; doi: 10.5483/bmbrep.2013.46.5.196. <https://www.ncbi.nlm.nih.gov/pubmed/23710639>.

Figures

Figure 1

Phase contrast image of human neuroblastoma SH-SY5Y cells under a light inverted microscope at 4x (left panel, scale bar = 100 mm) and 20x (right panel, scale bar = 50 mm) magnification (**a**). Microscopic images of the *B. mandrillaris* trophozoites cocultured with human neuroblastoma SH-SY5Y cells at 4x (left panel, scale bar = 100 mm) and 20x (right panel, scale bar = 50 mm) magnifications (**b**). Higher-magnification views are displayed in the insets in Fig. 1B. Scale bar = 25 mm (**c**). Trypan blue-stained human neuroblastoma SH-SY5Y cells. Scale bar in the left panel = 50 mm; scale bar on the right side = 25 mm (**d**). Relative level of mRNA encoding human anti-apoptotic BCL2 and apoptotic BAX protein at 1 and 3 hours post coculture. The levels are the mean \pm SD of triplicate experiments (**e**). Microscopic image of *B. mandrillaris* trophozoites on day 3 of coculture with the monolayer of human neuroblastoma SH-Sy5Y cells (**f**).

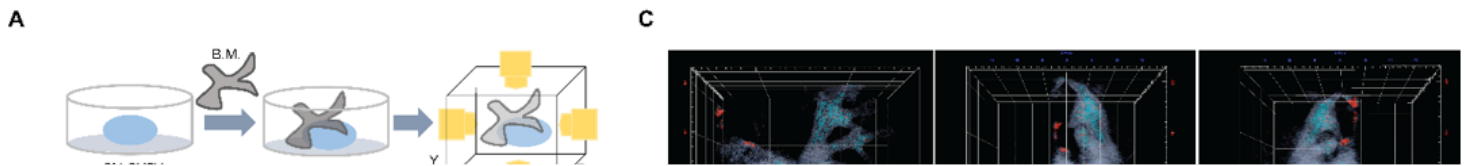


Figure 2

Schematic diagram of 3D imaging of cell-to-cell interactions using a holotomographic microscope (a). The 3D images of pseudocolored cells along the X-Y, X-Z and Y-Z planes are shown in the panels from left to right (b). X-Y view of the *B. mandrillaris* trophozoites interacting with human neuroblastoma SH-SY5Y cells (left panel), and the cytoplasmic bridge (arrows in the middle and right panel) in the Y-Z plane (c). B.M., *B. mandrillaris*; SH-SY5Y, human neuroblastoma cell line.

Figure 3

Schematic diagram of the differential cell tracking of CMFDA-labeled human neuroblastoma cells (green) and DiD-labeled *B. mandrillaris* trophozoites (magenta), followed by coculture (a). Cell-to-cell interactions of the DiD-labeled trophozoites (magenta) with human SH-SY5Y cells (green for CMFDA and blue for DAPI) at 40 min post coculture (b). Invadopodia of the *B. mandrillaris* trophozoites protruding into human neuroblastoma cells (c). The X-Y-Z plane of confocal images of the DiD-labeled trophozoites (magenta) with human SH-SY5Y cells (green for CMFDA and blue for DAPI) (d). Schematic diagram of the cellular uptake of unlabeled *B. mandrillaris* trophozoites (e). Confocal images of the *B. mandrillaris* trophozoites along the X-Y plane (f). Proportion of *B. mandrillaris* trophozoites that ingested human cell components (magenta circles) (g). PFA, paraformaldehyde.

Figure 4

Live imaging of CMFDA-labeled human neuroblastoma SH-SY5Y cells (green) cocultured with nonlabeled *B. mandrillaris* trophozoites using a holotomographic microscope (**a**). Snapshot images of CMFDA-labeled human neuroblastoma SH-Sy5Y cells (green). Insets show higher-magnification images captured with a 60x objective lens. Dotted lines indicate *B. mandrillaris* trophozoites (**b**). Schematic diagram of the cellular uptake of unlabeled *B. mandrillaris* trophozoites (**c**). Wortmannin-mediated inhibition of trogocytosis and cell ingestion by *B. mandrillaris* trophozoites (**d**).

Supplementary Files

This is a list of supplementary files associated with this preprint. Click to download.

- [Additionalfile1InvertedmicroscopeofBM24hmodified.mp4](#)
- [Additionalfile2Tomocubeimage008.mp4](#)
- [Additionalfile3Tomocubeimage018.mp4](#)
- [Addtionalfile4Tomocubeimage010.mp4](#)
- [Additionalfile53Dconfocal.mp4](#)
- [Addtionalfile6Tomocubeliveimage.mp4](#)
- [FigureS1.png](#)
- [FigureS2.png](#)
- [FigureS3.png](#)
- [GraphicalAbstract.png](#)